Texture Segmentation in 2D vs. 3D: Did 3D Developmentally Precede 2D?

Sejong Oh and Yoonsuck Choe
Department of Computer Science
Texas A&M University
3112 TAMU, College Station, TX 77843-3112
{sejong,choe}@tamu.edu

Abstract

Texture boundary detection (or segmentation) is an important capability in human vision. Usually, texture segmentation is viewed as a 2D problem, as the definition of the problem itself assumes a 2D substrate. However, an interesting hypothesis emerges when we ask a question regarding the nature *of textures:* What are textures, and why did the ability to discriminate texture evolve or develop? *A possible answer to this question is that textures naturally define physically distinct surfaces, thus, we can hypothesize that 2D texture segmentation may be an outgrowth of the ability to discriminate surfaces in 3D. In this paper, we investigated the relative difficulty of learning to segment textures in 2D vs. 3D configurations. It turns out that learning is faster and more accurate in 3D, very much in line with our expectation. Furthermore, we have shown that the learned ability to segment texture in 3D transfers well into 2D texture segmentation, bolstering our initial hypothesis, and providing a possible explanation for the developmental origin of 2D texture segmentation function in human vision.*

1. Introduction

Detection of a tiger in the bush is a perceptual task that carries a life or death consequence for preys trying to survive in the jungle [1]. Here, figure-ground separation becomes an important perceptual skill. Figure-ground separation is based on many different cues such as luminance, color, texture, etc. In case of the tiger in the jungle, texture plays a critical role. What are the visual processes that enable perceptual agents to separate figure from ground using texture cues? This intriguing question leads many researchers in vision to investigate the mechanisms of texture perception.

Beck[2][3] and Julesz[4] conducted psychological experiments investigating the features that enable humans to discriminate one texture from another. These studies suggested that texture segmentation occurs based on the distribution of simple properties of "texture elements", such as brightness, color, size, and the orientation of contours, or other elemental descriptors [5]. Julesz also proposed the texton theory, in which textures are discriminated if they differ in the density of simple, local textural features, called textons [6]. Most models based on these observations lead to a feature-based theory, in which segmentation occurs when feature differences (such as difference in orientation) exist. Furthermore, psychophysical and physiological studies have shown that human texture processing may be based on the detection of texture boundaries between heterogeneous textures using contextual influences via intra-cortical interactions in the primary visual cortex [7][8].

In the current studies of texture segmentation and boundary detection, texture is usually defined to be a 2D problem. However, an interesting hypothesis arises when we ask an important question regarding the nature of textures: *What are textures, and why did the ability to discriminate textures evolve or develop?* One possible answer to the question is that texture is that which defines physically distinct surfaces, belonging to different objects, and that texture segmentation function may have evolved out of the necessity to distinguish different surfaces. Human visual experience with textures in life can be, therefore, in most cases to use them as cues for surface perception, depth perception, and 3D structure perception. In fact, psychological experiments by Nakayama and He [9][10] showed that the visual system cannot ignore information regarding surface layout in texture discrimination and proposed that surface representation must actually precede perceptual functions such as texture perception (see the discussion section for more on this point).

From the discussion above, we can reasonably infer that texture processing may be closely related to surface discrimination. Surface discrimination is fundamentally a 3D task, and 3D cues such as stereopsis and motion parallax provide unambiguous information about the surface. Thus, we can hypothesize that 3D surface perception could have contributed in the formation of early texture segmentation processing capabilities in human vision. In this paper, through computational experiments using artificial neural networks, we investigate the relative difficulty of learning to discriminate texture boundaries in 2D vs. 3D arrangements of textures. We will also study whether the learned ability to segment texture in 3D can transfer into 2D. In the following, we will first describe in detail the methods we used to prepare the 2D and 3D texture inputs (Section 2.1), and the procedure we followed to train multilayer perceptrons to discriminate texture boundaries (Section 2.2). Next, we will present our main results and interpretations (Section 3), followed by discussion (Section 4) and conclusion (Section 5).

2. Methods

To test our hypothesis proposed in the introduction, we need to conduct texture discrimination experiments with 2D and 3D arrangements of textures. In this section, we will describe in detail how we prepared the two different arrangements (Section 2.1), and explain how we trained two standard multi-layer perceptrons to discriminate these texture arrangements (Section 2.2). We trained two separate networks that are identical in structure, one with input prepared in a 2D arrangement (we will refer to this network the *2D-net*), and the other in a 3D arrangement (the *3D-net*).

2.1. Input preparation

We prepared three sets of texture stimuli S_1, S_2, and S_3. Textures in S_1 were simple artificial texture images (oriented bars of orientation $0, \frac{\pi}{4}, \frac{\pi}{2}$, or $\frac{3\pi}{4}$); those in S_2 were more complex texture images (bars with orientations different from S_1 or more complex patterns such as crosses and circles); and those in S_3 were real texture images from the widely used Brodatz texture collection [11], as shown in Figure 1. For the training of the 2D-net and the 3D-net, four simple texture stimuli in S_1 were used. For testing the performance of the 2D-net and the 3D-net, all sets of texture stimuli, S_1, S_2 and S_3, were used.

To extract the primitive features in a given texture, we used Gabor filters. Previous results have shown that Gabor filters closely resemble experimentally measured receptive fields in the visual cortex [12] and have been widely used to model the response of visual cortical neurons. A number of texture analysis studies also used oriented Gabor filters or difference of Gaussian (DOG) filters to extract local image features [13][14].

We used a bank of oriented Gabor filters to approximate the responses of simple cells in the primary visual cortex.

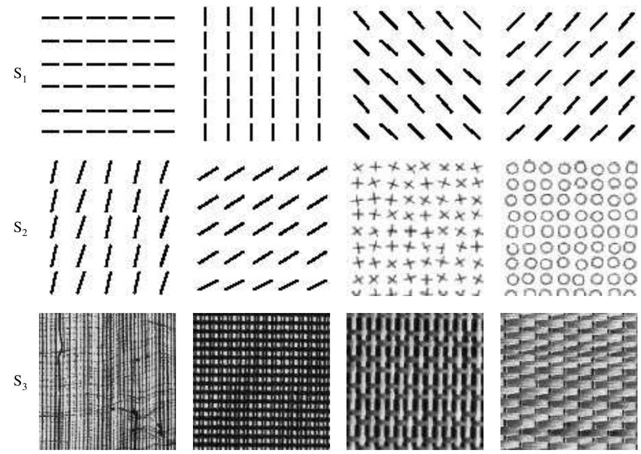

Figure 1. Texture stimuli. Three texture sets S_1, S_2, and S_3 are shown from the top row to the bottom.

The Gabor filter is defined as follows [15]:

$$G_{\theta,\phi,\sigma,\omega}(x, y) = \exp^{-\frac{x'^2+y'^2}{2\sigma^2}} \cos(2\pi\omega x' + \phi), \quad (1)$$

where θ is the orientation, ϕ is the phase, σ is the standard deviation (width) of the envelope, ω is the spatial frequency, (x, y) represents the pixel location, and x' and y' are defined as:

$$x' = x\cos(\theta) + y\sin(\theta) \quad (2)$$
$$y' = -x\sin(\theta) + y\cos(\theta). \quad (3)$$

For simplicity, only four different orientations ($0, \frac{\pi}{4}, \frac{\pi}{2}, \frac{3\pi}{4}$) were used for θ. (Below, we will refer to $G_{\theta,\phi,\sigma,\omega}$ as simply G.) To adequately sample the spatial-frequency features of input stimuli, three frequency ranges (1 to 3 cycles/degree) were used for ω. The size of filter was 16×16, $\sigma = 16/3$, and $\phi = \pi/2$. This resulted in 12 filters G_i (for $i = 1..12$) for the computation of simple cell responses as shown in Figure 2. To get the Gabor response matrix C_i, a gray-level intensity matrix I was obtained from the images randomly selected from S_1 and convolved with the filter bank G_i:

$$C_i = I * G_i, \quad (4)$$

where $i = 1..12$ denotes the index of a filter in the filter bank, and $*$ represents the convolution operator. The Gabor filtering stage is linear, but models purely based on linear mechanisms are not able to reproduce experimental data [16]. Thus, half-wave rectification is commonly used to provide a nonlinear response characteristic following linear filtering. However, in our experiments, full-wave rectification was used as in [17], which is similar to half-wave rectification, but is simpler to implement. Full-wave rectification is equivalent to summing the outputs of the two corresponding half-wave rectification channels (see, e.g. Bergen

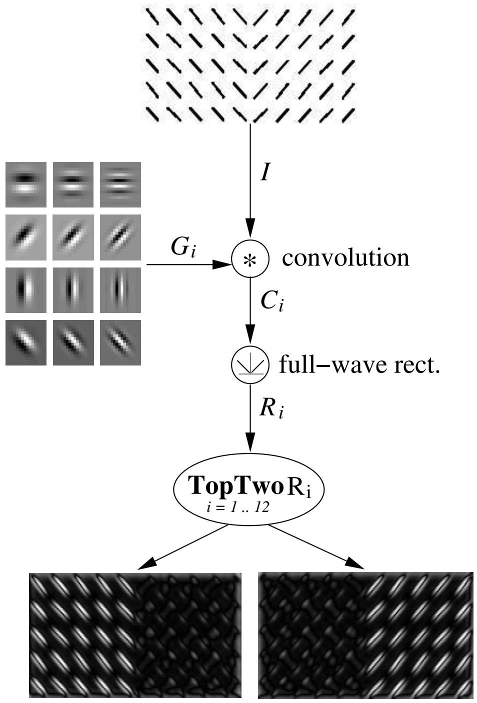

Figure 2. Gabor filter bank. The process used to generate two orientation response matrices is shown. The texture I is first convolved with the Gabor filters G_i (for $i = 1..12$), and the resulting responses are passed through a full-wave rectifier resulting in R_i. Finally, among the twelve R_is, two that showed maximal response are selected (bottom row; white is high and black is low response).

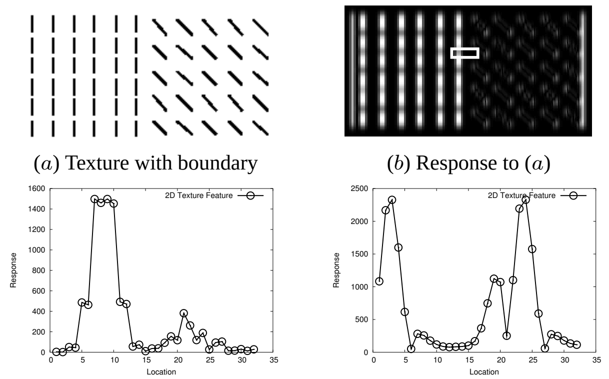

(a) Texture with boundary (b) Response to (a)

(c) Response profile of (b) (d) Response profile (no-boundary)

Figure 3. Generating the 2D input set (2D preprocessing). The procedure used to generate training data is shown. (a) Input with a texture boundary. (b) Orientation response calculated from (a). (c) The response profile from the 32-pixel wide area marked with a white rectangle in (b). (d) A similarly calculated response profile in a different input texture, for an area without a texture boundary (note the periodic peaks).

and Adelson [18] [16]). The final full-waved rectified Gabor feature response matrix is calculated as

$$R_i = |C_i|, \tag{5}$$

for $i = 1..12$. Among the twelve responses, only the top two maximally responding matrices were used in subsequent experiments. The same filtering procedure was used for both the 2D and the 3D arrangement of textures, which will be discussed below. Figure 2 shows the Gabor filter bank and the two maximally responding R_i's G_4 and G_{10} that have orientation preference of $\frac{\pi}{4}, \frac{3\pi}{4}$ and frequency of 1 cycle/degree.

To get the 2D training samples for the 2D-net, two randomly selected textures from S_1 were paired and convolved with the Gabor filter bank (figure 2). Only the two maximally responding ones from the 12 different response matrices were used as shown in figure 2. Each training input in the 2D training set consisted of a 32-element vector (say, ξ_k^{2D}, where k is the training sample index) taken from a horizontal strip (response profile) of the Gabor response matrix, and a single scalar value (say, ζ_k^{2D}) indicating the existence ($= 1$) or nonexistence ($= 0$) of a texture boundary within that strip. Each 32-element vector ξ_k^{2D} was taken from a horizontal strip centered at (x_c, y_c) within the response matrix (e.g., the white rectangle in figure 3b), where x_c is the horizontal center where the two textures meet, and y_c is randomly chosen within the full height of the matrix. When the two selected textures are the same, a texture boundary will not occur at the center, and if they were different a texture boundary will occur. We made sure that the number of input-target pair (ξ_k^{2D},ζ_k^{2D}) in each class, i.e., boundary vs. no boundary, was balanced. Figure 3c shows an example vector ξ_k^{2D} when there was a texture boundary, and figure 3d a case without a boundary.

For the training samples for the 3D-net, motion parallax was applied to simulate self-motion of an observer as shown in figure 4. One texture from a pair of textures was overlayed on top of the other and the texture above was allowed to slide over the one below, which resulted in successive further occlusion of the texture below. The texture above was moved by one pixel 32 times and each time the resulting 2D image (I'_j, for $j = t_1...t_{32}$; figure 5a) was convolved with the oriented Gabor filter bank followed by full-wave rectification as in the 2D preprocessing case (figure 5b). To generate a single training input pair (ξ_k^{3D}, ζ_k^{3D}) for the 3D-net, at each time step the response value from pixel (x_c, y_c) was collected into a 32-element vector, where x_c was 16 pixels away to the right from the initial texture boundary in the middle, and y_c was selected randomly for each new input pair but remained the same within the same input pair (the white square in figure 5b shows an example). Figure 5c shows an example of such a vector $\xi_k^{3\text{D}}$ (note that the x-axis represents time) for a case containing a texture boundary, and figure 5d a case without a boundary. The target value $\zeta_k^{3\text{D}}$ of the input pair ($\xi_k^{3\text{D}}, \zeta_k^{3\text{D}}$) was set in a similar manner as in the 2D case, either to 0 (no boundary) or 1 (boundary).

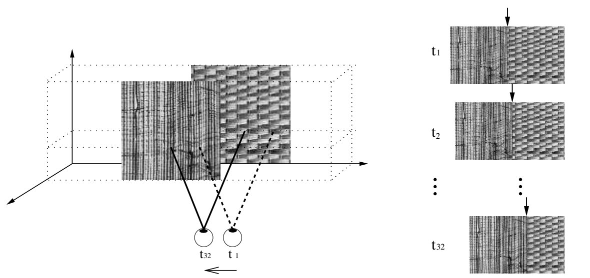

(a) Texture in 3D (b) Resulting 2D view

Figure 4. Generating the 3D input set (3D preprocessing). (a) A 3D configuration of textures and (b) the resulting 2D views before, during, and after the movement are shown. As the viewpoint is moved from the right to the left (t_1 to t_{32}) in 32 steps, the 2D texture boundaries in (b) (marked by black arrows) show a subtle variation.

For a fair comparison between the 2D and the 3D arrangements, 400 training samples were collected for each combination of two different textures to make 2,400 samples with target value of 1, and the same number of samples with target value of 0. This resulted in 4,800 input-target samples for each case (*1* $\leq$ *k* $\leq$ *4,800*). These 4,800 input-target samples from each training set were then randomly ordered during training.

2.2. Training the texture segmentation networks

We used standard multilayer perceptrons to perform texture boundary detection. The networks (2D-net and 3D-net), which consisted of two layers including 32 input units, 16 hidden units and 1 output unit, were trained for 1,000 epochs each using standard backpropagation with momentum (the learning rate was 0.2 and the momentum parameter was 0.9).[1] The goal of this study was to compare the relative learnability of the 2D vs. the 3D texture arrangements, thus a backpropagation network was good enough for our purpose. The input vectors were only drawn from the texture set S_1.

[1]Matlab neural networks toolbox was used for the simulations.

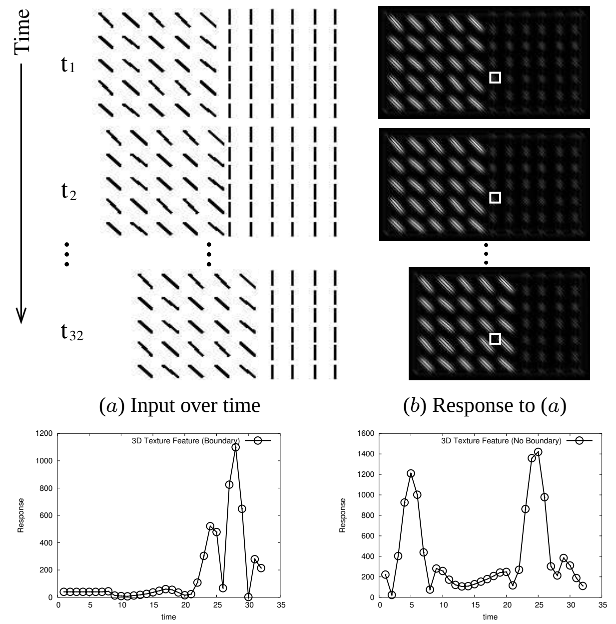

(a) Input over time (b) Response to (a)

(c) Temporal profile of (b) (d) Temporal profile (no boundary)

Figure 5. Generating 3D input set through motion (3D preprocessing). (a) Texture pair images resulting from simulated motion: I'_j for each $j = t_1..t_{32}$. (b) The response matrix of the texture pair: R_{ij}^{3D}. (c) Response profile obtained over time near the boundary of two different texture images (marked by the small squares). (d) A similarly measured response profile collected over time, using a different input texture, near a location without a texture boundary (note the periodic peaks).

After the two networks were trained, the speed of convergence and the classification accuracy were compared. To test generalization and transfer potentials, test stimuli drawn from the texture sets S_1, S_2, and S_3 were preprocessed using both 2D- and 3D-preprocessing to obtain six input sets. These input samples were then presented to the 2D-net and the 3D-net to compare the performances of the two networks.

3. Experiments and Results

We compared the performance of the two trained networks (2D-net and 3D-net), and also compared the performance of the two networks over novel texture images that were not used in training the networks.

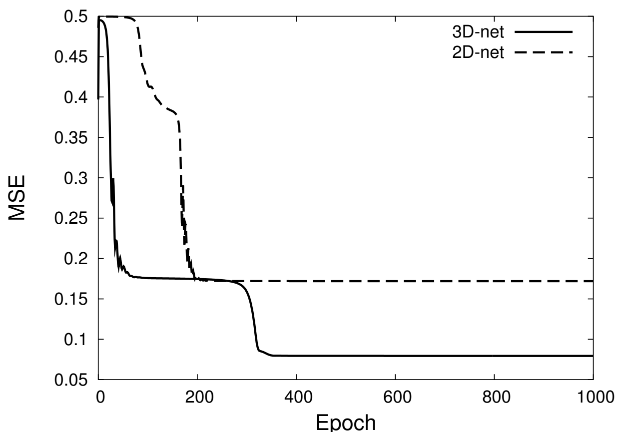

Figure 6. Learning curve of the networks. The learning curves of the 2D-net and the 3D-net after 1,000 epochs of training on texture set S_1 are shown. The 3D-net converges much faster than the 2D-net (near 50 epochs), suggesting that the 3D preprocessed training set may be easier to learn than the 2D set.

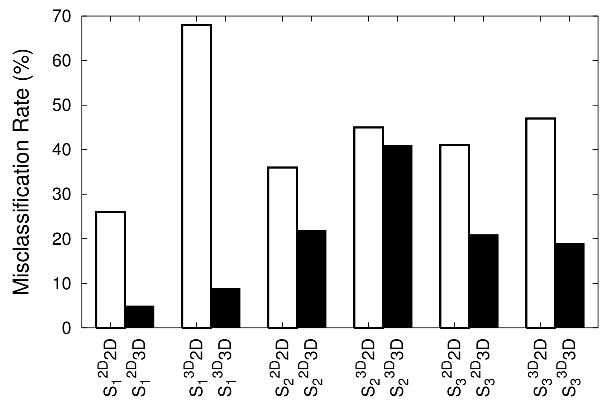

Figure 7. Comparison of misclassification rates. The misclassification rates of the different test conditions are shown (white bars represent the 2D-net, and the black bars the 3D-net). The x-axis label $S_i^{nD}mD$ indicates that input set i preprocessed in n-D was used as the test input, and the m-D network was used to measure the performance. In all cases, the 3D-net shows a lower misclassification rate compared to that of the 2D-net.

3.1. Speed of convergence and accuracy on the training set

Figure 6 shows the learning curves of two networks. After 1,000 epochs, the mean square error (MSE) of the 2D-net was 0.17 and that of the 3D-net was 0.08. A noticeable difference in the two learning curves is that the error rapidly decreases in the 3D-net (near 50 epochs), and the error at that moment is comparable already to the asymptotic error (~ 0.17) in the 2D-net. These results indicate that the 3D-net is easier to train than the 2D-net. In other words, texture arrangements in 3D may be easier to segment than those in 2D. We independently conducted 10 similar experiments, and the results were comparable each time (data not presented here). The misclassification rate in the 2D-net for the 2D training set was 26% and that of the 3D-net for the 3D training set was 9%, thus, accuracy was also higher in the 3D-net for the training data.

3.2. Generalization and transfer

The 2D-net and the 3D-net trained with the texture set S_1 were tested on texture pairs from S_1, S_2 and S_3. (Note that for the texture set S_1, input vectors different from those in the training set were used.) The test samples were prepared in the same manner as the training samples, which gave us three 4,000-sample sets of 2D and three 4,000-sample sets of 3D per each texture set. All six sample sets were presented to the 2D-net and the 3D-net. We used two methods to compare the performance of the networks. First, we compared the misclassification rate, which is the percentage of misclassification. Misclassification rates were calculated for all 12 cases (= 6 sample sets $\times$ 2 networks): Figure 7 shows the result. The 3D-net outperformed the 2D-net in all cases, even for the sample set from S_1 with 2D preprocessing, which was similar to those used for training the 2D-net. It is also notable that the 3D-net outperformed the 2D-net on all the sample sets prepared with 2D preprocessing (1st, 3rd, and the 5th column in figure 7; these are basically a 2D texture segmentation problem), where one would normally expect the 2D-net to perform better because of the manner in which the input was prepared. These results suggest that (1) developing a texture segmentation function in 3D can be easier than in 2D, and (2) the ability to segment texture in 3D may transfer very well into solving texture segmentation problems in 2D.

As another measure of performance, we compared the absolute error ($= |target - output|$) for each test case for the two networks. The results are shown in figure 8. The plot shows the mean absolute errors and their 99% confidence intervals. The results are comparable with those reported above: The 3D-net consistently outperformed the 2D-net, and the differences were found to be statistically significant (t-test: $n = 4,000, p << 0.001$), except for one case (S_2 with 3D preprocessing; figure 8 fourth pair from the left).

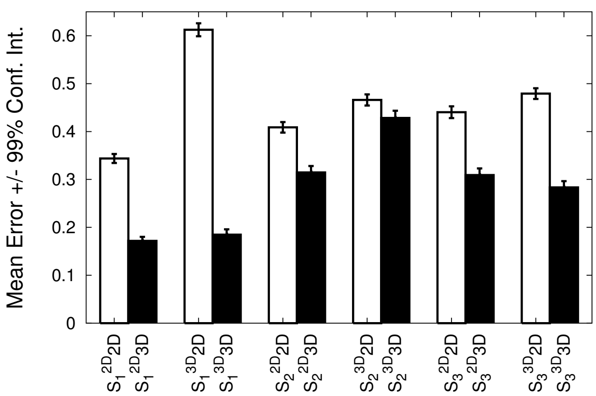

Figure 8. Comparison of output errors. The mean error in the output vs. the target value in each trial and its 99% confidence interval (error bars) are shown for all test cases (white bars represent the 2D-net, and the black bars the 3D-net). In all cases except for the fourth pair from the left (S_2^{3D}2D and S_2^{3D}3D), the differences between the 3D-net and the 2D-net are significant (t-test: $n = 4,000, p << 0.001$).

4. Discussion

Since the early works of Julesz[4] and Beck[2] on texture perception, a lot of studies have been conducted to understand the mechanisms of the human visual system underlying texture segmentation and boundary detection in both psychophysical research and pattern recognition research. In most cases their main concerns have been about the texture perception ability of human in 2D. The present paper suggests an alternative approach to the problem of texture perception, with a focus on boundary detection. First, we demonstrated that texture boundary detection in 3D is easier than in 2D. We also showed that the learned ability to find texture boundary in 3D can easily be transferred to texture boundary detection in 2D. Based on these results, our careful observation is that the outstanding ability of 2D texture boundary detection of the human visual system may have been derived from an analogous ability in 3D.

Our preliminary results allow us to challenge one common belief that many other texture boundary detection studies share. In this view, intermediate visual processing such as texture perception, visual search and motion process do not require object (in our context, “3D”) knowledge, and thus perform rapidly; and texture perception is understood in terms of features and filtering, so the performance is determined by differences in the response profiles of receptive fields in low-level visual processing. A similar point as ours was advanced by Nakayama and his colleagues [9][10]. In Nakayama’s alternative view on intermediate visual processing, visual surface representation is necessary before other visual tasks such as texture perception, visual search, and motion perception can be accomplished (figure 9). Such an observation is in line with our results indicating that 3D performance can easily transfer into a 2D task.

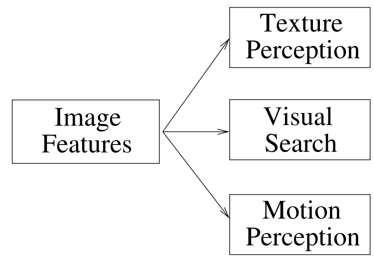

(a) Traditional view

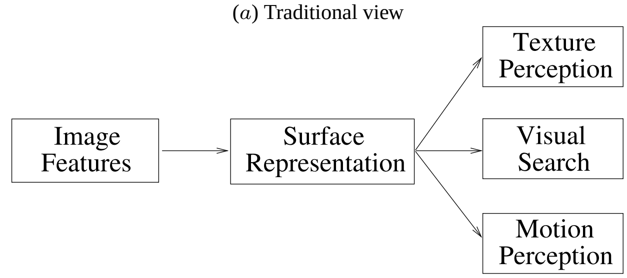

(b) An alternative view

Figure 9. Two views of intermediate visual processing. (a) Texture perception, visual search, motion perception depend on feature processing in early cortical areas. (b) Surface representation must precede intermediate visual tasks [10]. Adapted from [10].

The main goal of our work was to understand the nature of textures, and from that emerged the importance of 3D cues in understanding the texture detection mechanism in human visual processing. To emulate 3D depth, we employed motion cues to provide 3D depth. This imposes potential limitations on our work, which is that additional information in 3D input may have become available to the 3D-net–some form of temporal information that that 2D inputs do not have. This can be seen as an unfair advantage for the 3D-net, but on the other hand, the 2D-net has additional spatial information which the 3D-net does not have, so eventually these two relative advantages may cancel out.

5. Conclusion

We began with the simple question regarding the nature of textures. The tentative answer was that textures naturally define distinct physical surfaces, and thus the ability to segment texture in 2D may have grown out of the ability to distinguish surfaces in 3D. To test our insight, we compared texture boundary detection performance of two neural networks trained on textures arranged in 2D and in 3D. Our results revealed that texture boundary detection in 3D is easier to learn than in 2D, and that the network trained in 3D easily solved the 2D problem as well, but not the other way around. Based on these results, we carefully conclude that the human ability to segment texture in 2D may have originated from a module evolved to handle 3D tasks. One immediate future direction is to extend our current approach to utilize stereo cues as well as monocular cues used in this paper.

Acknowledgments

This research was supported by the Texas Higher Education Coordinating Board ATP #000512-0217-2001, and by the National Institute of Mental Health Human Brain Project #1R01-MH66991.

References

[1] M. Tuceryan, *The Handbook of Pattern Recognition and Computer Vision*, 2nd ed. World Scientific Publishing Co., 1998, ch. 2.1 Texture Analysis, pp. 207–248.

[2] J. Beck, "Effect of orientation and of shape similarity on grouping," *Perception and Psychophysics*, pp. 300–302, 1966.

[3] ——, "Textural segmentation, second-order statistics and textural elements," *Biological Cybernetics*, vol. 48, pp. 125–130, 1983.

[4] B. Julesz, "Texture and visual perception," *Scientific American*, vol. 212, pp. 38–48, Feb 1965.

[5] M. S. Landy and N. Graham, *The Visual Neurosciences*. MIT Press, 2004, ch. Visual perception of texture, pp. 1106–1118.

[6] B. Julesz and J. Bergen, "Texton theory of preattentive vision and texture perception," *Journal of the Optical Society of America*, vol. 72, 1982.

[7] Thielscher and Neumann, "Neural mechanisms of cortico-cortical interaction in texture boundary detection: a modeling approach," *Neuroscience.*, vol. 122, no. 4, pp. 921–39, 2003.

[8] Z. Li, "Pre-attentive segmentation in the primary visual cortex," *Spatial Vision*, vol. 13, no. 1, pp. 25–50, 2000.

[9] Z. J. He and K. Nakayama, "Perceiving textures: beyond filtering," *Vision Research*, vol. 34(2), pp. 151–62, 1994.

[10] K. Nakayama, Z. J. He, and S. Shimojo, *Visual Cognition*, 2nd ed. MIT Press, 1995, ch. Visual Surface Representation: A Critical Link between Lower-level and Higher-level vision, pp. 1–70.

[11] P. Brodatz, *Textures: A Photographic Album for Artists and Designer*. New York: Dover Publication, 1966.

[12] J. P. Jones and L. A. Palmer, "An evaluation of the two-dimensional gabor filter model of simple receptive fields in cat striate cortex," *Journal of Neurophysiology*, vol. 58, no. 6, pp. 1223–1258, 1987.

[13] I. Fogel and D. Sagi, "Gabor filters as texture discriminator," *Biological Cybernetics*, vol. 61, pp. 102–113, 1989.

[14] A. Bovik, M. Clark, and W. Geisler, "Multichannel texture analysis using localized spatial filters," *IEEE Transactions on Pattern Analysis and Machine Intelligence*, vol. 12, no. 1, pp. 55–73, January 1990.

[15] J. Daugman, "Two-dimensional spectral analysis of cortical receptive field profiles," *Vision Research*, vol. 20, pp. 847–856, 1980.

[16] J. Malik and P. Perona, "Preattentive texture discrimination with early vision mechanisms," *Journal of Optical Society of America A*, pp. 923–932, 1990.

[17] J. R. Bergen and E. H. Adelson, "Early vision and texture perception," *Nature*, vol. 333, pp. 363–364, May 1988.

[18] J. Bergen and M. Landy, "Computational modeling of visual texture segregation," 1991.